Adsorption (2011) 17: 21–26
DOI 10.1007/s10450-010-9281-7

Methane adsorption in PIM-1

Gregory S. Larsen · Ping Lin · Flor R. Siperstein · Coray M. Colina

Received: 13 May 2010 / Accepted: 8 October 2010 / Published online: 22 October 2010
© Springer Science+Business Media, LLC 2010

Abstract We report the results of Grand Canonical Monte Carlo (GCMC) simulations of methane adsorption in a prototypical polymer of intrinsic microporosity, PIM-1. Polymer chains were represented with a united-atom model, with Lennard-Jones parameters obtained from the TraPPE potential. Additionally, partial charges were calculated from *ab initio* methods using Gaussian (HF/6-31G* basis set). Samples of PIM-1 were built at low density conditions, followed by a Molecular Dynamics compression protocol until densities of 1.2 g cm^{-3} were achieved. This protocol proved to be suitable for the realistic modeling of the amorphous structure of PIM-1. Surface areas and pore size distributions were measured and compared to available experimental data. The simulated pore size distribution present a peak at 4.3 Å, consistent with experimental results. GCMC simulations of methane adsorption were performed, and found to qualitatively reproduce the shape of the available experimental isotherm.

Keywords Polymers of intrinsic microporosity · PIMs · Simulation · Adsorption · GCMC · MD

G.S. Larsen · C.M. Colina (✉)
Department of Materials Science and Engineering, The Pennsylvania State University, 320 Steidle, University Park, PA, 16802, USA
e-mail: colina@matse.psu.edu

P. Lin
The Materials Simulation Center, The Pennsylvania State University, University Park, PA, 16802, USA

F.R. Siperstein
School of Chemical Engineering and Analytical Science, University of Manchester, Manchester, M13 9PL, UK

1 Introduction

Microporous materials, defined by the IUPAC as systems with pores less than 2 nm in size, are useful in applications such as gas storage, separations, purification, and heterogeneous catalysis. Microporous materials include zeolites, activated carbons, and more recently, metal and covalent organic frameworks (Morris and Wheatley 2008; Côté et al. 2005). Polymers of intrinsic microporosity (PIMs) (McKeown and Budd 2006) are a new class of porous polymer based on the simple design principle of combining monomers that are both rigid and non-planar or non-linear. These structural conditions inhibit space efficient packing and give the polymers their microporosity, but put no limitation on the chemical structure of the monomers. The wide variety of chemistries combined with the high surface areas make PIMs a promising material for a variety of applications.

Computer simulations comprise a powerful set of tools that have found many applications in the study of adsorbent materials (Duren et al. 2009). Classical, forcefield based, molecular dynamics (MD) and Monte Carlo (MC) simulations are particularly well suited to study physical adsorption which is dominated by van der Waals and electrostatic interactions. This allows the exploration of real and hypothetical materials at an atomistic level of detail difficult to achieve experimentally. In this work, we utilize MD and MC simulations to increase our understanding of methane adsorption in the prototypical PIM, PIM-1, with the greater goal of using this knowledge to aid in the rational design of novel PIMs.

In this work, we use computer simulations to study the adsorption behavior of methane in PIM-1. The rest of the paper is organized as follows. In Sect. 2 we present the details of the preparation of our model PIM-1, and details of

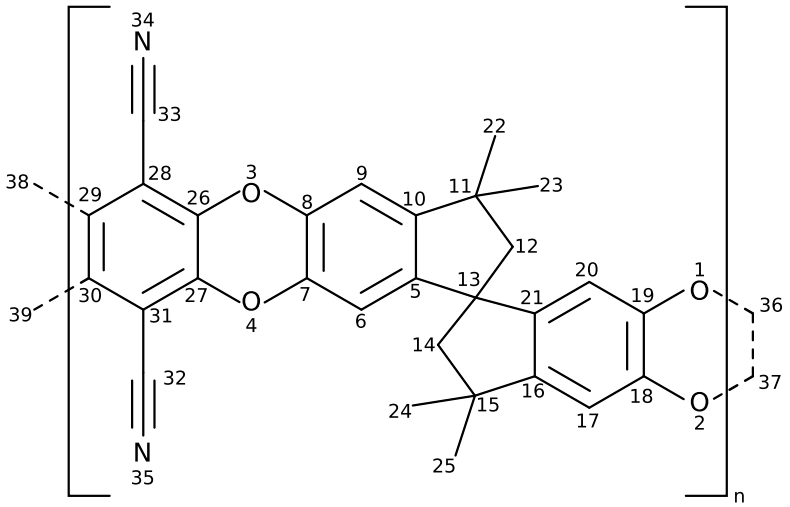

Fig. 1 The chemical structure for PIM-1 showing the characteristic rigid backbone and site of contortion, here developed by the ladder like fused aromatic ring structures and spirobisindane moiety. Note the atoms (36–39) that cap the chain ends are zero charge pseudo atoms used to mitigate chain end effects. Each atom or pseudo atom number have Lennard-Jones parameters, partial charges, and associated references given in Table 1

our simulations for gas adsorptions. Then, in Sect. 3, we present and compare our simulated adsorption isotherms and pore size distributions with available experimental results. Finally some concluding remarks and suggestions for future work are given.

2 Methods

The approach taken in this work to build realistic simulation samples of PIM-1 is to grow a system at a low density, chain by chain, then compress the system via MD to achieve realistic densities. Chains are randomly initiated throughout the simulation box and grown by randomly choosing one of the two chiral monomers and one of the two possible orientations until the target chain length of 10 monomers is achieved or an overlap is the result of adding either monomer type in either orientation. This results in systems of roughly 100 monomers in 10 to 14 chains (for low density box sizes of 100 Å). Similar systems have also been studied by Heuchel et al. (2008). During the chain growth process, no attempt to move the chains or minimize the system energy is made. To limit the effect of chain ends on chain packing and adsorption, zero charge blocking atoms are placed at the head and tail of each chain, as shown in Fig. 1. Given the large, low density sample, an equilibration cycle consisting of several short NVT and NPT MD simulations were performed. The twelve step equilibration cycle follows that of Karayiannis et al. (2004) with pressures of 1000, 3000, and 5000 atmospheres and a final NPT equilibration step at 1 atmosphere lasting 300 ps. MD simulations use the Nosé-Hoover thermostat and barostat and were performed with LAMMPS (Plimpton 1995).

As specific interactions with hydrogens were not expected to be significant, this work uses a united atom model in which the hydrogen atoms are grouped with the carbon to which they are bonded. Lennard-Jones (LJ) parameters were taken from the TraPPE potential. While the TraPPE united atom model is in general well suited to describing the system, it does not have adequate parameters to describe the oxygens atoms within a ring or the aromatic carbons connected to the oxygens. Therefore, those parameters were taken from the all atom TraPPE-EH model.

In order to assign partial charges to the monomers, a quantum mechanics calculation for a monomer model in the gas phase at the HF/6-31G* level of theory using Gaussian 03 (Frisch et al. 2004) was carried out. The model monomer used in the ab initio calculations is defined as the repeating structure between two spirocenters (split at the 5 member rings rather than the 6 member aromatic rings). Capping methyl groups were placed on the joint carbon (number 13 in Fig. 1) between two five member rings. Afterward, a two-stage restrained electrostatic potential (RESP) (Cornell et al. 1995) charge fitting to the electrostatic potential was performed to obtain the partial charges. This approach and the level of theory selected have been shown to perform well for condensed phase simulations by other groups (Cornell et al. 1995). All LJ parameters and partial charges are listed in Table 1 with atom numbers corresponding to Fig. 1.

Sample densities, surface areas (SA), and pore size distributions (PSD) were measured for characterization and comparison to available experimental data. The simulated and experimental densities are measured differently and are related by the pore volume per unit mass by the following relation:

$$\frac{1}{\rho_{sim}} = \frac{1}{\rho_{exp}} + \frac{v_{pore}}{g_{sample}} \tag{1}$$

where ρ_{sim} is the simulation density, ρ_{exp} is the experimental or skeletal density, v_{pore} is the pore volume and g_{sample} is the sample mass (see further discussion below). The accessible SA of the simulation samples were measured by

Table 1 Simulation parameters for PIM-1, atom numbers corresponding to Fig. 1

Pseudo atom number	Atom group[a]	Charge (eV)[a]	ϵ (K)[a]	σ (Å)[b]	Reference
1, 2, 3, 4	C(aro)-**O(aro)**-X(aro)	−0.219064	70	2.60	Rai and Siepmann (2007)
5, 10, 16, 21	R-**C(aro)**	0.038356	21	3.88	Wick et al. (2000)
28, 31	R-**C(aro)**	−0.12304	21	3.88	Wick et al. (2000)
6, 9, 17, 20	CH(aro)	−0.124962	50.5	3.695	Wick et al. (2000)
7, 8, 18, 19	X(aro)-**C(aro)**-X(aro)	0.373561	30.7	3.60	Rai and Siepmann (2007)
26, 27, 29, 30	X(aro)-**C(aro)**-X(aro)	0.172261	30.7	3.60	Rai and Siepmann (2007)
36, 37	X(aro)-**C(aro)**-X(aro)	0	30.7	3.60	Rai and Siepmann (2007)
22, 23, 24, 25, 38, 39	CH_3	0	98	3.75	Martin and Siepmann (1999)
11, 13, 15	C	0.0979454	0.5	6.4	Martin and Siepmann (1999)
12, 14	CH_2	−0.016466	51	3.89	Lee et al. (2005)
32, 33	C(sp, nitrile)	0.313718	60	3.55	Wick et al. (2005)
34, 35	N(nitrile)	−0.40999	60	2.95	Wick et al. (2005)

[a]From the TraPPE potential

[b]From *ab initio*, this work

Monte Carlo integration as described by Duren et al. (2007) in which a nitrogen sized probe molecule ($\sigma = 3.681$ Å) is randomly inserted around each of the framework atoms in turn and checked for overlap with other framework atoms. The fraction of non-overlapping probe molecules is then used to calculate the accessible SA. The PSD is derived from the fractional free volume (FFV). The simulation sample is overlaid with a fine, three dimensional grid, each node of which is marked as occupied or unoccupied by the polymer. Test probes of decreasing diameter are placed at each node. The fraction of unoccupied space accessible to probes that do not overlap with the polymer matrix are summed, giving the FFV as a function of probe diameter. The negative derivative of the FFV with respect to the probe diameter gives the PSD (Gelb and Gubbins 1999).

After compression, relaxation, and characterization, simulations of gas adsorption were performed. Simulations were run in the Grand Canonical ensemble using the MC-CCS Towhee code (Martin and Siepmann 1999). Chemical potentials were calculated for methane by the ideal gas relation:

$$\mu = k_B T \ln\left(\frac{P\Lambda^3}{k_B T}\right) \tag{2}$$

where k_B is the Boltzmann's constant, T is the temperature in K, P is the pressure, and Λ is the de Broglie wavelength. Experimentally the polymer sample has been observed to swell slightly upon the adsorption of methane ($\frac{\Delta V}{V_0} = 1.94\%$ Hölck 2008). Thus, as a first approximation in this work, we have held the polymer matrix fixed and rigid during the adsorption simulations. Simulations were run for at least 3×10^7 steps at each pressure. At pressures of 1 bar and less, the system equilibrated from the empty state in less than 1.5×10^6 steps. At higher pressures, the output from each pressure step was used as the input for the next ensuring equilibration within 1.5×10^6 steps.

3 Results and discussion

As the number of computations increases rapidly with the number of particles in the simulation, it is desirable to use as small of a sample as possible. This tendency towards smaller samples needs to be balanced such that the size of the sample does not affect the simulation results (Frenkel and Smit 2002; Allen and Tildesley 1989). Because adsorptive properties are heavily dependent on SA and PSD, the optimal sample size was determined by comparing the SA and PSD for ten samples of 32, 45, and 55 Å which were compressed, as described above, from 70, 100, and 120 Å respectively. No significant variation in SA between individual samples or sample sizes was observed. As the PSD is the negative derivative of the FFV, differences between sample sizes are more easily seen in the FFV. In Fig. 2, we show the average FFV as a function of probe size for the three different sample sizes. There is a wide variability in FFV for the 32 Å samples with an average value much higher than that of the 45 and 55 Å samples. The FFV for the 45 and 55 Å samples have similar variability and are equivalent within error bars. Thus the 45 Å sample is chosen as the optimal box size.

Simulation samples were characterized by their density, SA, and PSD. Each of these quantities can be calculated from simulations and measured experimentally. However, a comparison between the simulation and experimental results requires care. For example, the key difference between simulation and experimental calculations of the density is that

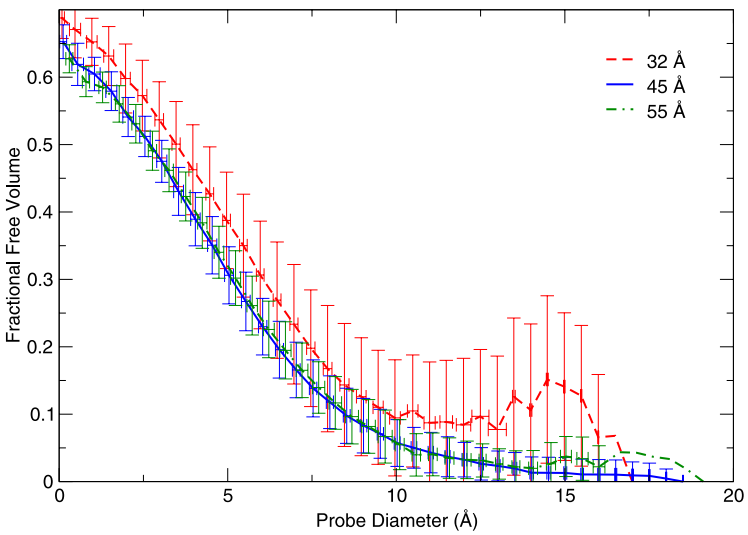

Fig. 2 Average fractional free volume of ten 32 (– –), 45 (—), and 55 (–···) Å samples as a function of probe diameter

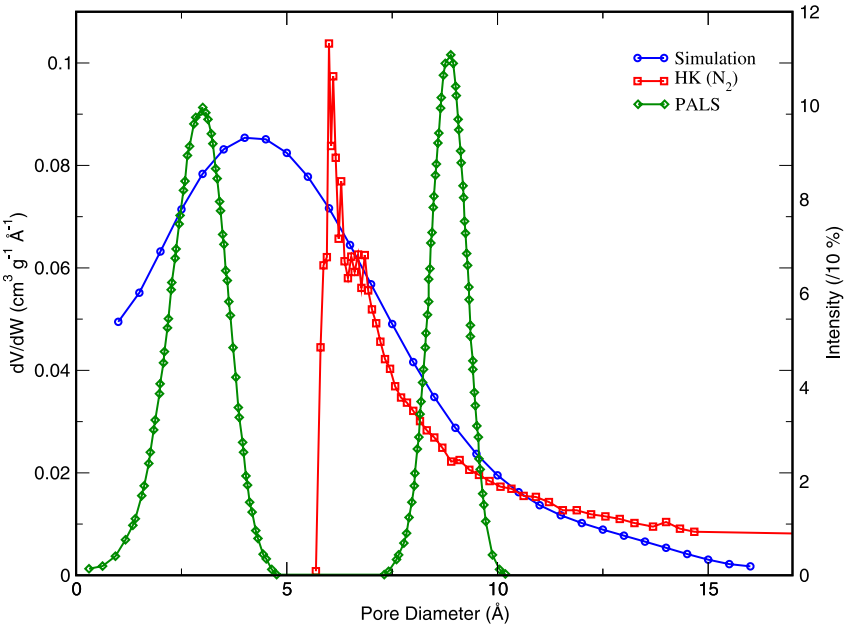

Fig. 3 Pore size distribution (PSD) from simulations (*circle*), the HK method (N_2 adsorption) (*square*) from Budd et al. (2005), and PALS (*diamond*) of Staiger et al. (2008)

experiments measure the skeletal volume while simulations use the total volume of the simulation box. Thus, the simulated and experimental densities differ by the pore volume according to (1). Experimentally, we measured the density of a powdered PIM-1 sample to be 0.94 g cm^{-3} via helium pycnometry (Larsen et al. 2010) while other works have measured a density of 1.06–1.09 g cm^{-3} in films via measurement of the sample weight in air and in the fluorocarbon fluid Fluorinert FC-77 (Budd et al. 2006), and 1.4 g cm^{-3} for films via helium pycnometry (Heuchel et al. 2008). From simulations of helium adsorption, the pore volumes for the 45 Å sample can be calculated as (Myers and Monson 2002):

$$v_g = \frac{n_{ads}}{\rho_{\mathrm{He}}} \tag{3}$$

where ρ_{He} is the density of helium at 1 bar, 20 °C, v_g is the pore volume per unit mass, and n_{ads} is the amount of He in the sample. The pore volume was calculated to be 0.3495 cm^3 g^{-1}. This corresponds to an experimental density of 1.21 g cm^{-3}.

The PSD is a derived quantity in both simulations and experiments, thus comparing PSDs from different methods is fraught with difficulties in reconciling the different techniques and their underlying assumptions. In Fig. 3, we show a plot of experimental PSDs derived from the Horvath-Kawazoe (HK) method (Budd et al. 2005), Positron Annihilation Lifetime Spectroscopy (PALS) (Staiger et al. 2008) and the simulated PSD for the 45 Å sample from the average FFV. The HK data are based on N_2 adsorption and the assumption that smaller pores fill at lower pressures. The low

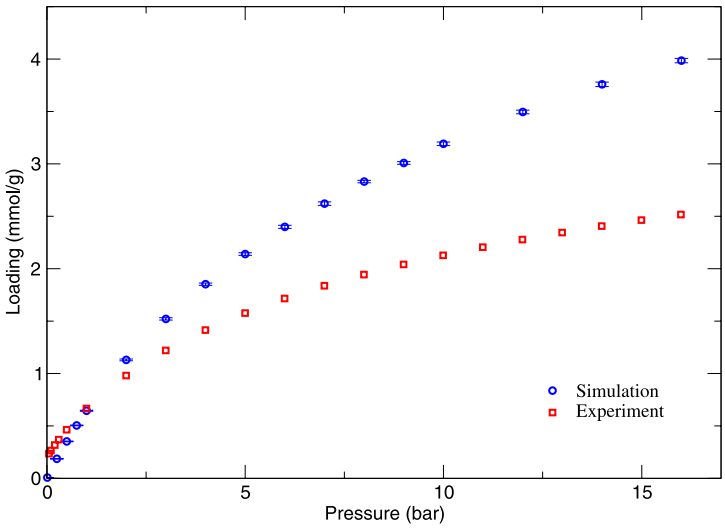

Fig. 4 Simulated (*circles*) and experimental (*squares*) adsorption isotherms for methane in PIM-1 at 20 °C as a function of pressure (*bar*)

pore size resolution limit is therefore determined by the low pressure limit of the device; the contribution of pores below this limit are grouped in with the first measurable pores creating an inflated peak near the limit of the instrument. The PALS data of Staiger et al. (2008) were interpreted as a bimodal PSD. The work of Staiger et al. (2008) also show PALS PSDs with slightly shifted peaks and peak heights depending on the age of the sample, storage method, and polymerization technique. This variability in reported PSDs as well as SAs and densities (see below), suggest that subtle differences in polymer history can affect the polymer structure making the target simulation sample structure poorly defined. However, the simulated PSD shows a peak at 4.3 Å, this is somewhat larger than the low PALS peak, and 2 Å smaller than the HK data. Given the experimental variability, our simulation sample is a reasonable approximation. It is also worth noting that the simulation samples have a finite range of pore sizes that extend no larger than 18 Å.

Surface areas for ten 45 Å boxes were calculated with an average value of 940.24 ± 126.297 $m^2\,g^{-1}$. Experimentally, PIM-1 is reported to have a BET surface area of 750 to 860 $m^2\,g^{-1}$ (Budd et al. 2004; Ghanem et al. 2008; McKeown et al. 2007). The deviation between simulated and experimental values can be attributed to the ideal nature of the simulation sample. It is likely that the experimental sample has residual solvent or other contamination present (Budd et al. 2008) as well as kinetically inaccessible pores that would decrease the apparent surface area.

After the sample was characterized, GCMC simulations of methane adsorption were performed. The simulated adsorption isotherm is plotted against the experimental isotherm for powdered PIM-1, (Larsen et al. 2010) in Fig. 4. The simulation qualitatively reproduces the shape of the isotherm with order of magnitude quantitative agreement. The difference between the simulated and experimental adsorption isotherms is probably due to three main factors. First, the experimental sample likely contains residual solvent or some other adsorbed contamination (Budd et al. 2008). Additional experimental measurements of gas adsorption in methanol treated (and non-treated) samples as well as further simulations will be valuable in assessing the effect of residual solvent and contamination. Second, different sample histories have been experimentally shown to cause minor variations in the pore size distributions (Staiger et al. 2008) suggesting that the unique "sample history" (compression and relaxation) from simulations will cause slightly different adsorptive behavior. Finally, there are likely kinetically inaccessible pores in the experimental sample that are still filled in simulations. Future work will look to investigate the proportion of inaccessible pores.

In this work we report molecular simulation results for methane adsorption on a united-atom model of PIM-1. A detailed investigation of the structure of other gases inside these pores, as well as similar PIMs with other functionalities, such as fluorine and aromatic nitrogen are currently underway in our group, and could be relevant for ongoing research in heterogeneous catalysis, purification, separations, and gas storage.

Acknowledgements The authors are grateful to Peter M. Budd for helpful discussions. We gratefully acknowledge funding from the Donors of the American Chemical Society Petroleum Research Fund for partial support of this research (48570-AC7) and the National Science Foundation (DMR-0908781). High performance computational resources for this research were provided by the Lion-HPC systems of Penn State ITS.

References

Allen, M.P., Tildesley, D.J.: Computer Simulation of Liquids. Clarendon Press, New York (1989)

Budd, P.M., Elabas, E.S., Ghanem, B.S., Makhseed, S., McKeown, N.B., Msayib, K.J., Tattershall, C.E., Wang, D.: Solution-processed, organophilic membrane derived from a polymer of intrinsic microporosity. Adv. Mater. **16**(5), 456–459 (2004)

Budd, P.M., McKeown, N.B., Fritsch, D.: Free volume and intrinsic microporosity in polymers. J. Mater. Chem. **15**(20), 1977–1986 (2005)

Budd, P.M., McKeown, N.B., Fritsch, D.: Polymers of intrinsic microporosity (PIMs): high free volume polymers for membrane applications. Macromol. Symp. **15**(20), 1977–1986 (2006)

Budd, P.M., McKeown, N.B., Ghanem, B.S., Msayib, K.J., Fritsch, D., Starannikova, L., Belov, N., Sanfirova, O., Yampolskii, Y., Shantarovich, V.: Gas permeation parameters and other physicochemical properties of a polymer of intrinsic microporosity: polybenzodioxane PIM-1. J. Membr. Sci. **325**(2), 851–860 (2008)

Cornell, W.D., Cieplak, P., Bayly, C.I., Gould, I.R., Merz, K.M., Ferguson, D.M., Spellmeyer, D.C., Fox, T., Caldwell, J.W., Kollman, P.A.: A second generation force-field for the simulation of proteins, nucleic-acids, and organic-molecules. J. Am. Chem. Soc. **117**(19), 5179–5197 (1995)

Côté, A.P., Benin, A.I., Ockwig, N.W., O'Keeffe, M., Matzger, A.J., Yaghi, O.M.: Porous crystalline, covalent organic frameworks. Science **310**(5751), 1166–1170 (2005)

Duren, T., Millange, F., Ferey, G., Walton, K.S., Snurr, R.Q.: Calculating geometric surface areas as a characterization tool for metal-organic frameworks. J. Phys. Chem. C **111**(42), 15,350–15,356 (2007)

Duren, T., Bae, Y.S., Snurr, R.Q.: Using molecular simulation to characterise metal-organic frameworks for adsorption applications. Chem. Soc. Rev. **38**(5), 1237–1247 (2009)

Frenkel, D., Smit, B.: Understanding Molecular Simulation, 2nd edn. Academic Press, London (2002)

Frisch, M.J., Trucks, G.W., Schlegel, H.B., Scuseria, G.E., Robb, M.A., Cheeseman, J.R., Montgomery, J.A. Jr., Vreven, T., Kudin, K.N., Burant, J.C., Millam, J.M., Iyengar, S.S., Tomasi, J., Barone, V., Mennucci, B., Cossi, M., Scalmani, G., Rega, N., Petersson, G.A., Nakatsuji, H., Hada, M., Ehara, M., Toyota, K., Fukuda, R., Hasegawa, J., Ishida, M., Nakajima, T., Honda, Y., Kitao, O., Nakai, H., Klene, M., Li, X., Knox, J.E., Hratchian, H.P., Cross, J.B., Bakken, V., Adamo, C., Jaramillo, J., Gomperts, R., Stratmann, R.E., Yazyev, O., Austin, A.J., Cammi, R., Pomelli, C., Ochterski, J.W., Ayala, P.Y., Morokuma, K., Voth, G.A., Salvador, P., Dannenberg, J.J., Zakrzewski, V.G., Dapprich, S., Daniels, A.D., Strain, M.C., Farkas, O., Malick, D.K., Rabuck, A.D., Raghavachari, K., Foresman, J.B., Ortiz, J.V., Cui, Q., Baboul, A.G., Clifford, S., Cioslowski, J., Stefanov, B.B., Liu, G., Liashenko, A., Piskorz, P., Komaromi, I., Martin, R.L., Fox, D.J., Keith, T., Al-Laham, M.A., Peng, C.Y., Nanayakkara, A., Challacombe, M., Gill, P.M.W., Johnson, B., Chen, W., Wong, M.W., Gonzalez, C., Pople, J.A.: Gaussian 03, Revision C.02. Gaussian, Inc., Wallingford (2004)

Gelb, L.D., Gubbins, K.E.: Correlation functions of adsorbed fluids in porous glass: a computer simulation study. Mol. Phys. **96**(12), 1795–1804 (1999)

Ghanem, B.S., McKeown, N.B., Budd, P.M., Fritsch, D.: Polymers of intrinsic microporosity derived from bis(phenazyl) monomers. Macromolecules **41**(5), 1640–1646 (2008)

Heuchel, M., Fritsch, D., Budd, P.M., McKeown, N.B., Hofmann, D.: Atomistic packing model and free volume distribution of a polymer with intrinsic microporosity (PIM-1). J. Membr. Sci. **318**(1–2), 84–99 (2008)

Hölck, O.: Gas sorption and swelling in glassy polymers. PhD thesis, Berlin Institute of Technology (2008)

Karayiannis, N.C., Mavrantzas, V.G., Theodorou, D.N.: Detailed atomistic simulation of the segmental dynamics and barrier properties of amorphous poly(ethyleneterephthalate) and poly(ethylene isophthalate). Macromolecules **37**(8), 2978–2995 (2004)

Larsen, G.S., Siperstein, F.R., Budd, P.M., Colina, C.M.: Gas adsorption in PIM-1: CO_2 and CH_4 adsorption in polymer of intrinsic microporosity 1 (PIM-1). Ind. Eng. Chem. Res. (2010) (to be submitted)

Lee, J.S., Wick, C.D., Stubbs, J.M., Siepmann, J.I.: Simulating the vapour-liquid equilibria of large cyclic alkanes. Mol. Phys. **103**(1), 99–104 (2005)

Martin, M.G., Siepmann, J.I.: Novel configurational-bias Monte Carlo method for branched molecules. Transferable potentials for phase equilibria. 2. united-atom description of branched alkanes. J. Phys. Chem. B **103**(21), 4508–4517 (1999). URL http://towhee.sourceforge.net

McKeown, N.B., Budd, P.M.: Polymers of intrinsic microporosity (PIMs): organic materials for membrane separations, heterogeneous catalysis and hydrogen storage. Chem. Soc. Rev. **35**(8), 675–683 (2006)

McKeown, N.B., Budd, P.M., Book, D.: Microporous polymers as potential hydrogen storage materials. Macromol. Rapid Commun. **28**(9), 995–1002 (2007)

Morris, R.E., Wheatley, P.S.: Gas storage in nanoporous materials. Angew. Chem. Int. Ed. **47**(27), 4966–4981 (2008)

Myers, A.L., Monson, P.A.: Adsorption in porous materials at high pressure: theory and experiment. Langmuir **18**(26), 10,261–10,273 (2002)

Plimpton, S.J.: Fast parallel algorithms for short-range molecular dynamics. J. Comput. Phys. **117**(1), 1–19 (1995). URL lammps.sandia.gov

Rai, N., Siepmann, JI: Transferable potentials for phase equilibria. 9. explicit hydrogen description of benzene and five-membered and six-membered heterocyclic aromatic compounds. J. Phys. Chem. B **111**(36), 10,790–10,799 (2007)

Staiger, C.L., Pas, S.J., Hill, A.J., Cornelius, C.J.: Gas separation, free volume distribution, and physical aging of a highly microporous spirobisindane polymer. Chem. Mater. **20**(8), 2606–2608 (2008)

Wick, C.D., Martin, M.G., Siepmann, J.I.: Transferable potentials for phase equilibria. 4. United-atom description of linear and branched alkenes and alkylbenzenes. J. Phys. Chem. B **104**(33), 8008–8016 (2000)

Wick, C.D., Stubbs, J.M., Rai, N., Siepmann, J.I.: Transferable potentials for phase equilibria. 7. Primary, secondary, and tertiary amines, nitroalkanes and nitrobenzene, nitriles, amides, pyridine, and pyrimidine. J. Phys. Chem. B **109**(40), 18,974–18,982 (2005)